Electronic Supplementary Material (ESI) for Journal of Materials Chemistry A.

Supporting Information

Flexible All-Solid-State Fiber-Shaped Ni-Fe Batteries with High Electrochemical Performance

Qiulong Li [+], Qichong Zhang[+], Chenglong Liu[+], Juan Sun, Jiabin Guo, Jun Zhang, Zhenyu Zhou, Bing He, Zhenghui Pan, Yagang Yao *

Materials

Cobalt nitrate hexahydrate ($Co(NO_3)_2 \cdot 6H_2O$, 98.5%), iron chloride hexahydrate ($FeCl_3 \cdot 6H_2O$, 99%), terephthalic acid ($C_8H_6O_4$, 99%), and PVA ($[CH_2CH(OH)]_n$, n = 1799) were purchased from Aladdin. Dimethyl formamide (DMF, C_3H_7NO, 99.5%), sodium hypophosphite ($NaH_2PO_2 \cdot H_2O$, 98%), ammonium fluoride (NH_4F, 96%), urea ($CO(NH_2)_2$, 99%), nickel sulfate hexahydrate ($NiSO_4 \cdot 6H_2O$, 98.5%), potassium persulfate ($K_2S_2O_8$, 99.5%), ammonia water ($NH_3 \cdot H_2O$, 28%), and potassium hydroxide (KOH, 85%) were obtained from Sinopharm Chemical Reagent, China. Each of these chemicals was used directly without any further purification. Carbon nanotube fibers (CNTFs) were fabricated with a floating catalyst chemical vapor deposition method followed by shrinking with ethanol.

Materials characterization

The morphology of the as-prepared samples was characterized by utilizing a scanning electron microscope (SEM) (Hitachi S-4800, 5 kV). The microstructure of the samples was observed by the transmission electron microscope (TEM) (Tecnai G2 F20 S-Twin) and the high-resolution TEM images were recorded on an FEI Tecnai G2 20 high-resolution transmission electron microscope at an acceleration voltage of 200 kV. The chemical composition of the samples was analyzed on an ESCALab MKII X-ray photoelectron spectrometer (XPS) with nonmonochromatized Mg Kα X-rays as the excitation source. X-ray diffraction (XRD) patterns were acquired with a Rigaku D/MAX2500 V with Cu Kα radiation (λ = 1.5418 Å).

Electrochemical Performance Measurements

The electrochemical performance of the fabricated samples was evaluated by galvanostatic charge/discharge (GCD), cyclic voltammetry (CV), and electrochemical impedance spectroscopy (EIS) measurements on an electrochemical workstation (CHI 760E, Chenhua) using a three-electrode configuration in 3 M KOH aqueous solution. The fabricated electrode materials, Pt wire and Ag/AgCl were used as the working, counter and reference electrodes, respectively. The EIS measurements were assumed between 10^{-2}-10^{5} Hz with a voltage amplitude of 5 mV and open-circuit potential. The capacity (C), energy density (E), and power density (P) were calculated according to the following equations:

$$C_A = \frac{1}{3600} \frac{I\Delta t}{A} \quad (1)$$

$$E_A = C_A * V_p \quad (2)$$

$$P_A = 3600 * \frac{EA}{\Delta t} \quad (3)$$

$$C_V = \frac{1}{3600} \frac{I\Delta t}{V} \quad (4)$$

$$E_V = C_V * V_p \quad (5)$$

$$P_V = 3600 * \frac{EV}{\Delta t} \quad (6)$$

Where A and V are the total area and volume of the as-assembled fiber-shaped energy storage devices (FESDs), respectively. I, Δt and V_p are the discharge current, discharge time, and voltage platform. The cycle life tests were conducted with GCD measurements with a constant current density of 30 mA/cm^2 for 3,000 cycles.

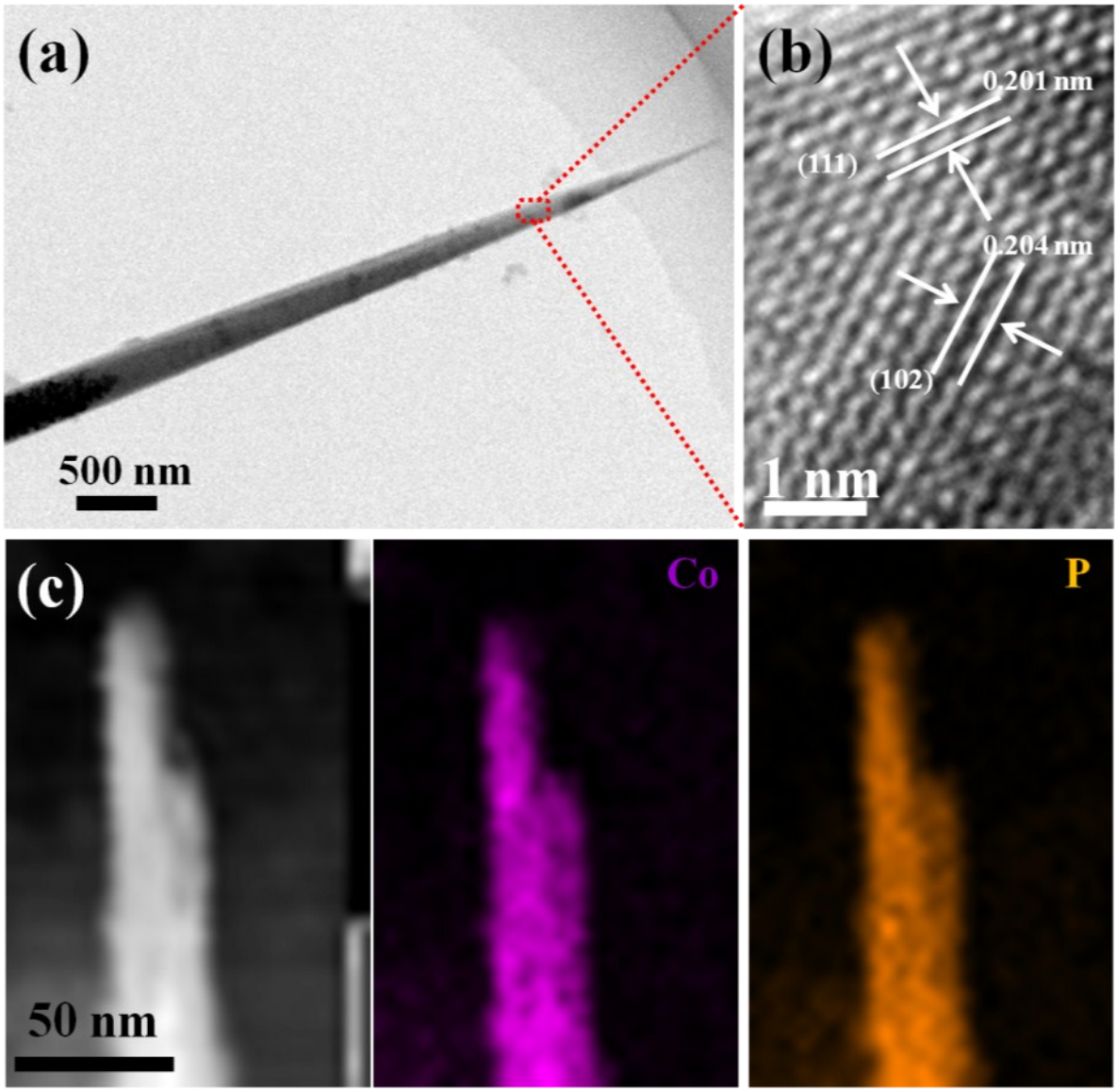

Figure S1 (a) Low-magnification TEM image of single CoP nanowire. (b) High-magnification of the red rectangle in panel a. (c) TEM image of the CoP nanowire and the corresponding EDS element mapping images.

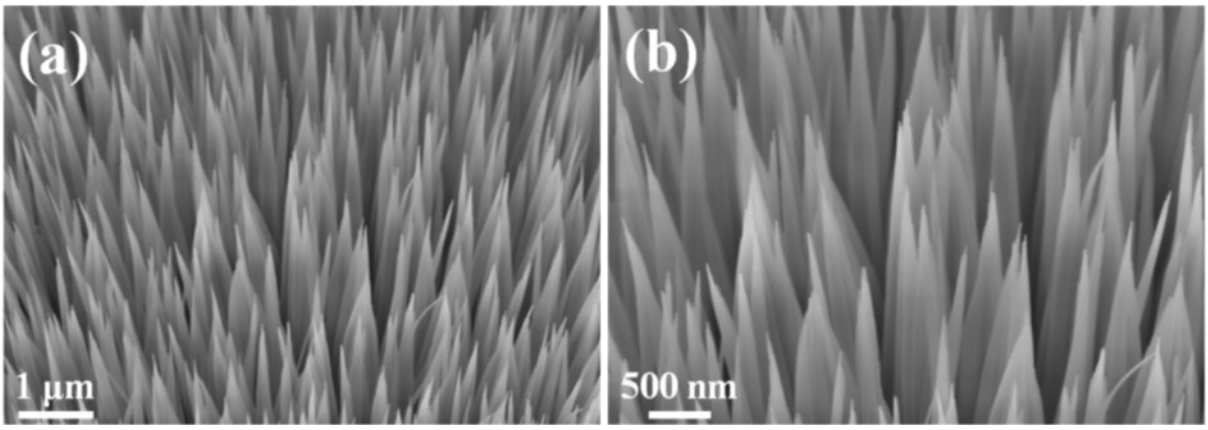

Figure S2 (a) and (b) SEM images of the Co_3O_4 NWAs/CNTF at different magnifications.

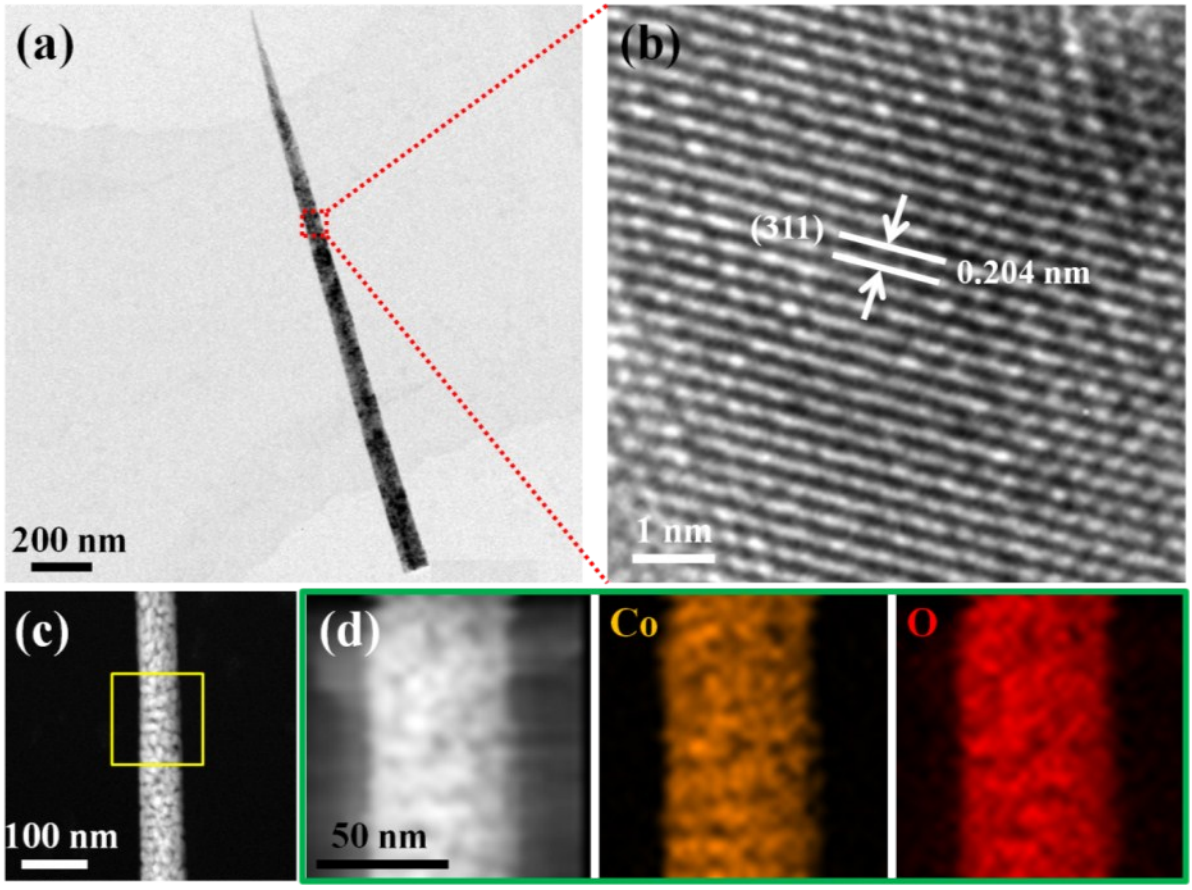

Figure S3 (a) Low-magnification TEM image of single Co_3O_4 nanowire. (b) High-magnification of the red rectangle in panel a. (c) TEM image of partially single Co_3O_4 nanowire. (d) TEM image and corresponding EDS element mapping images of the yellow rectangle in panel c.

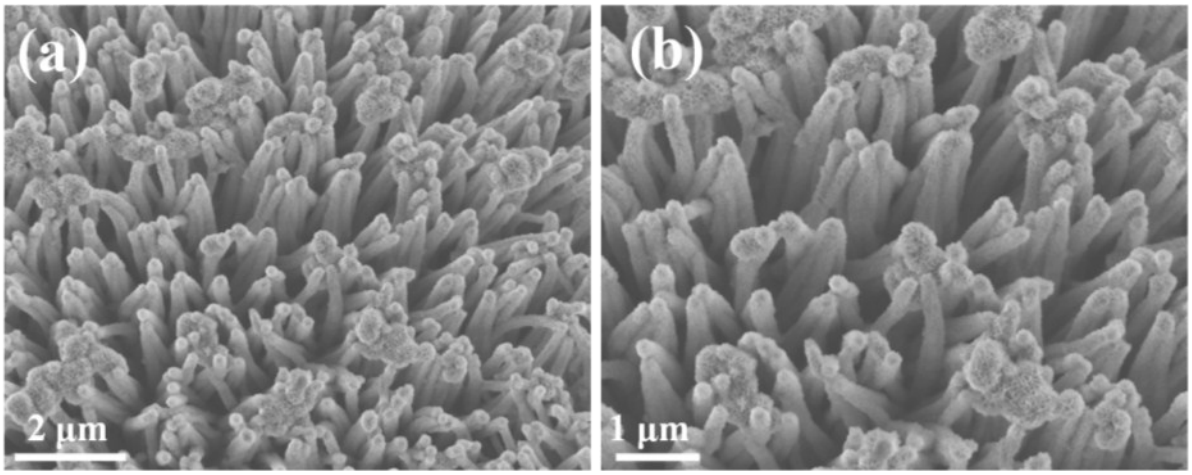

Figure S4 (a) and (b) SEM images of the Co_3O_4@$Ni(OH)_2$ NWAs/CNTF at different magnifications.

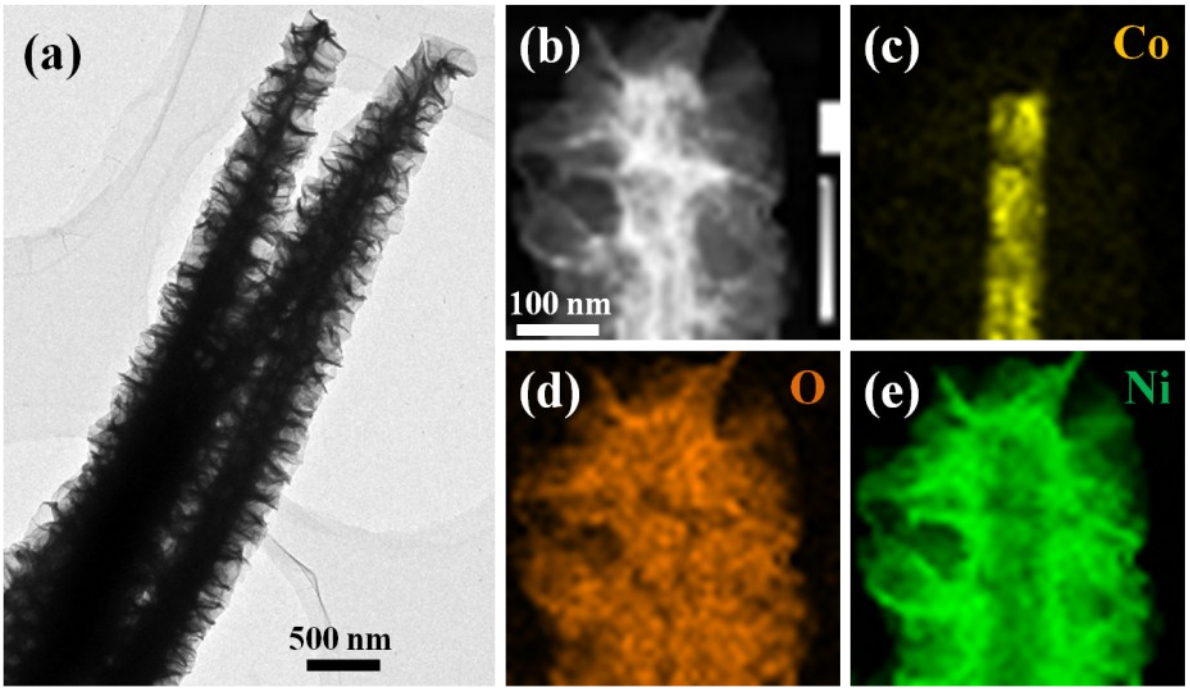

Figure S5 (a) Low-magnification TEM image of Co_3O_4@@$Ni(OH)_2$ NWAs. (b) STEM bright feld image of Co_3O_4@@$Ni(OH)_2$ NWAs. Elemental mapping of (c) Co, (d) O, and (e) Ni.

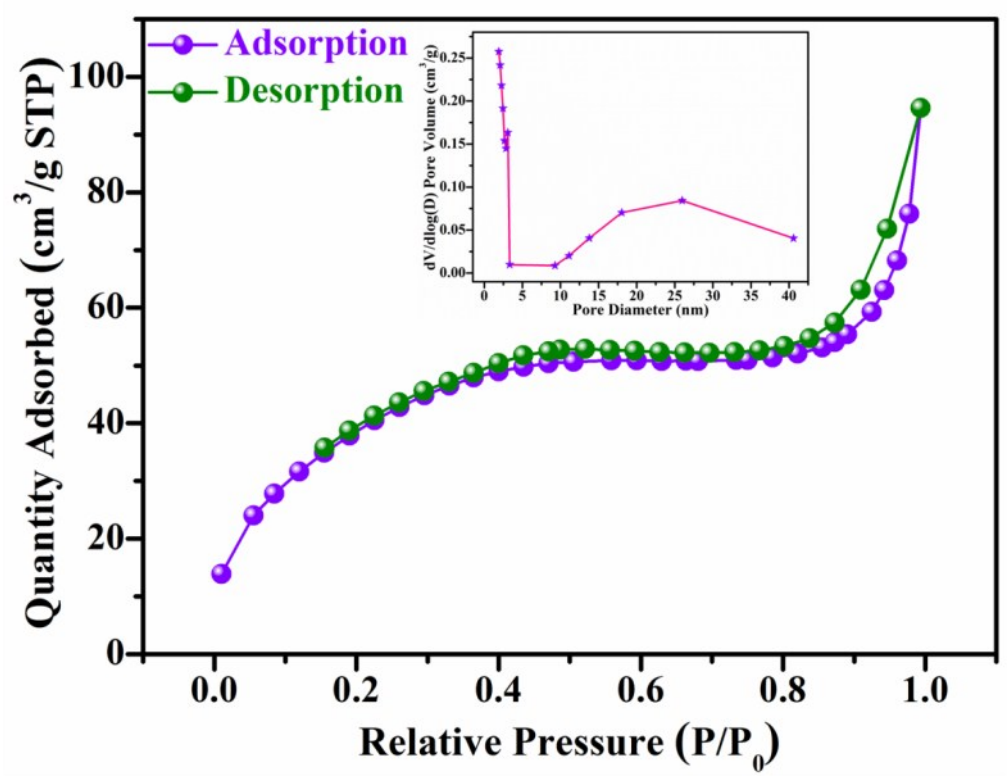

Figure S6 N_2 absorption-desorption isotherm of the CoP@$Ni(OH)_2$ NWAs/CNTF cathode material (Inset: BJH desorption pore distribution).

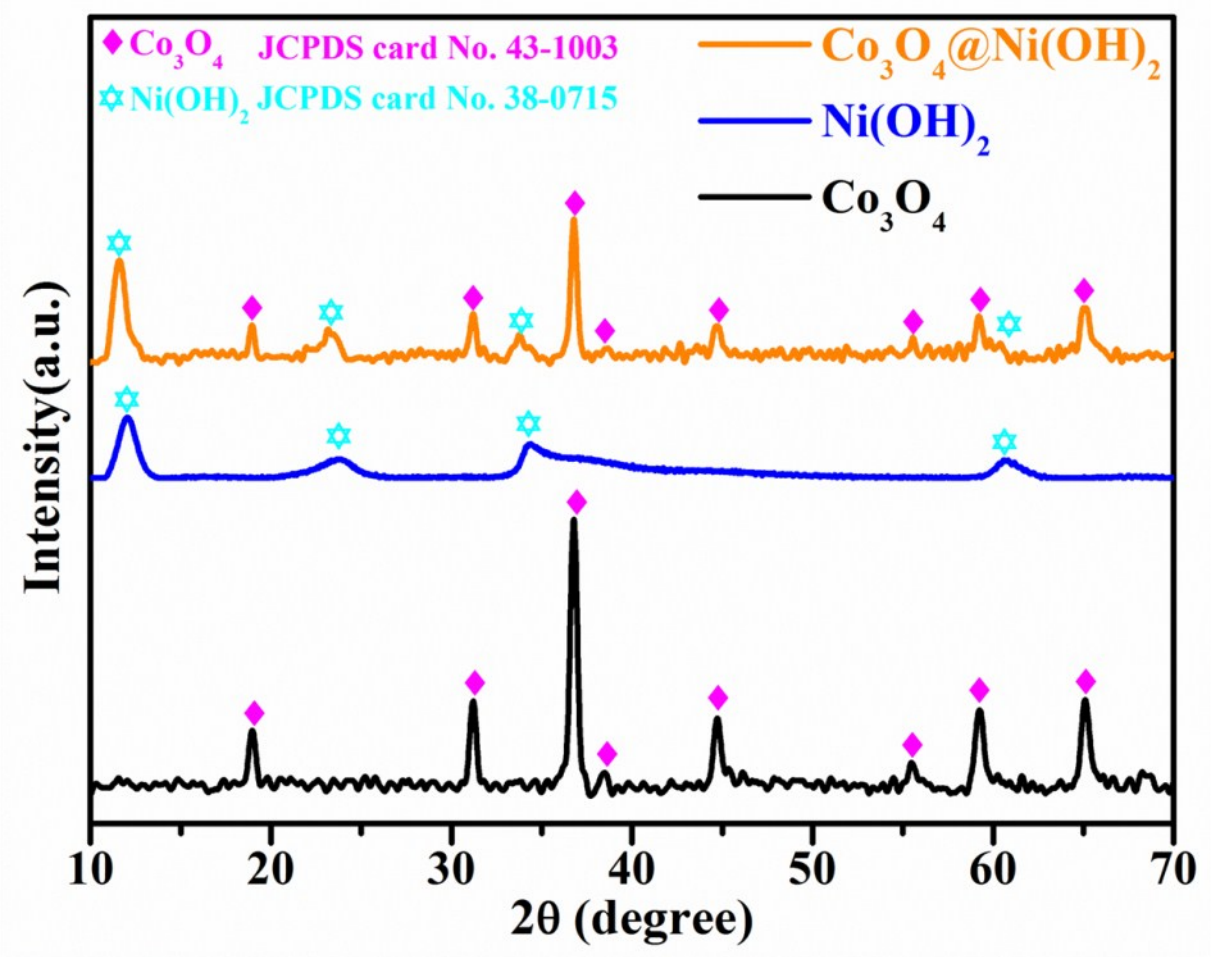

Figure S7 XRD patterns of Co_3O_4@$Ni(OH)_2$ NWAs, $Ni(OH)_2$ nanosheets and Co_3O_4 NWAs.

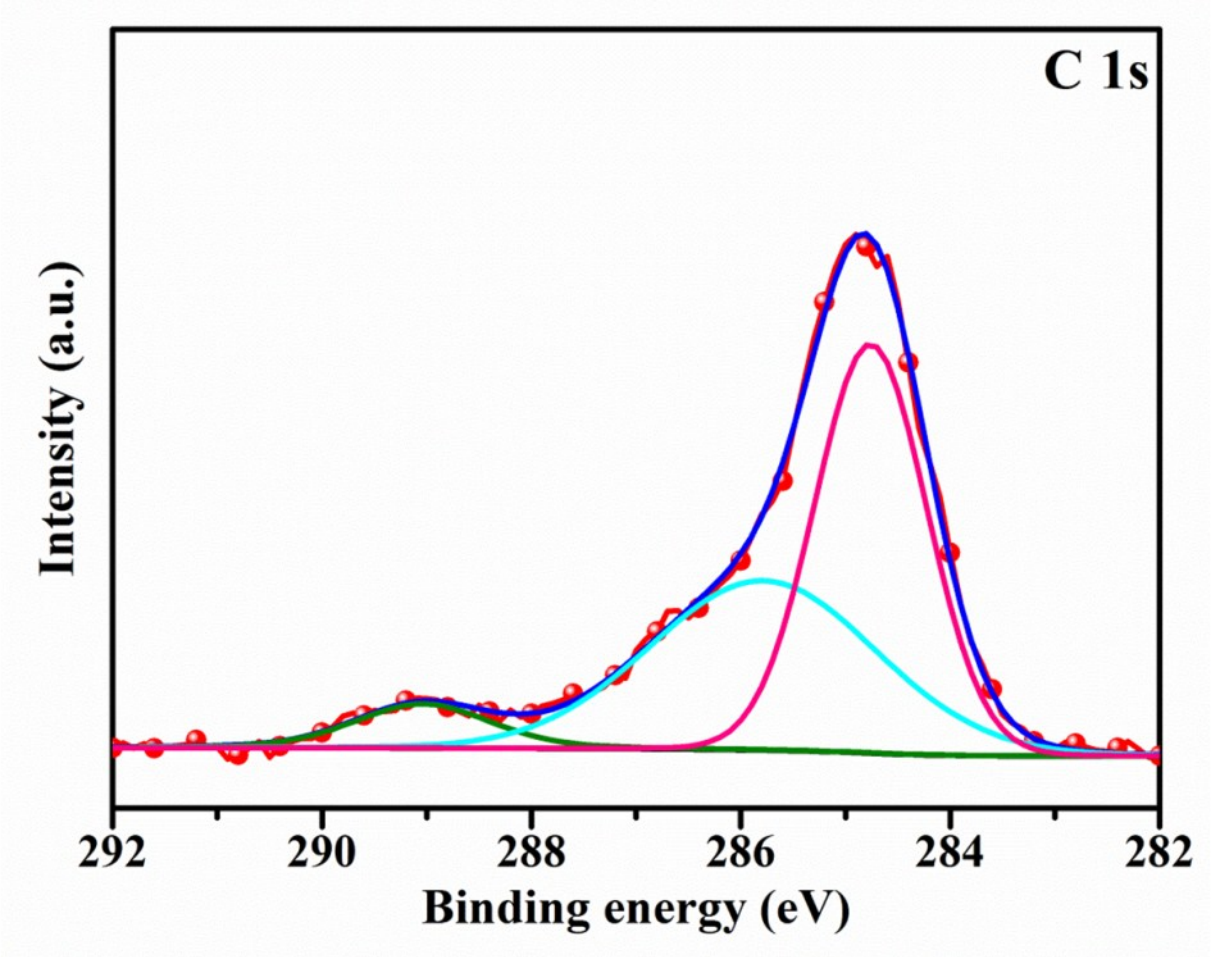

Figure S8 High-resolution C 1s XPS spectra of the CoP@Ni(OH)$_2$ NWAs/CNTF.

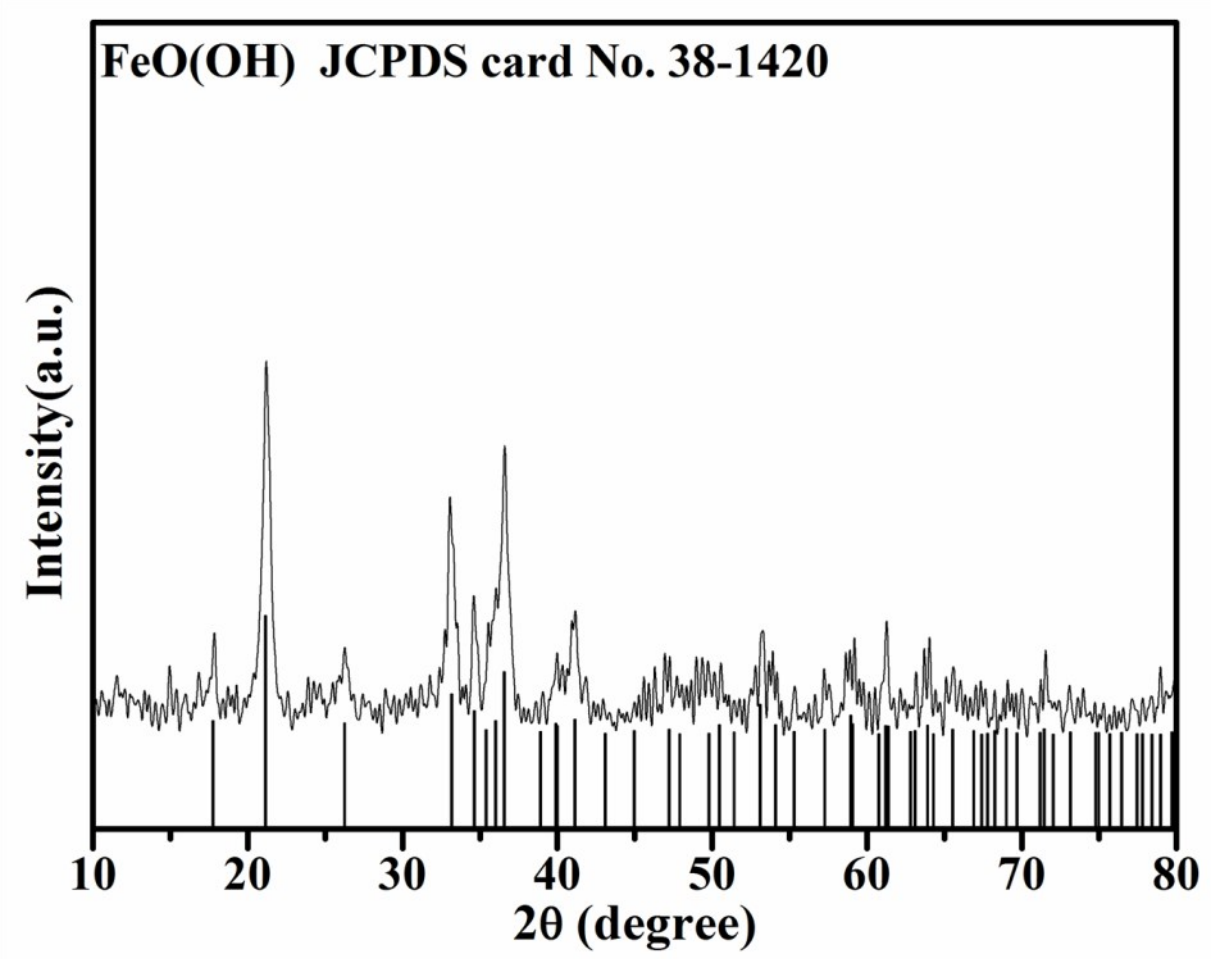

Figure S9 XRD spectra of FeO(OH).

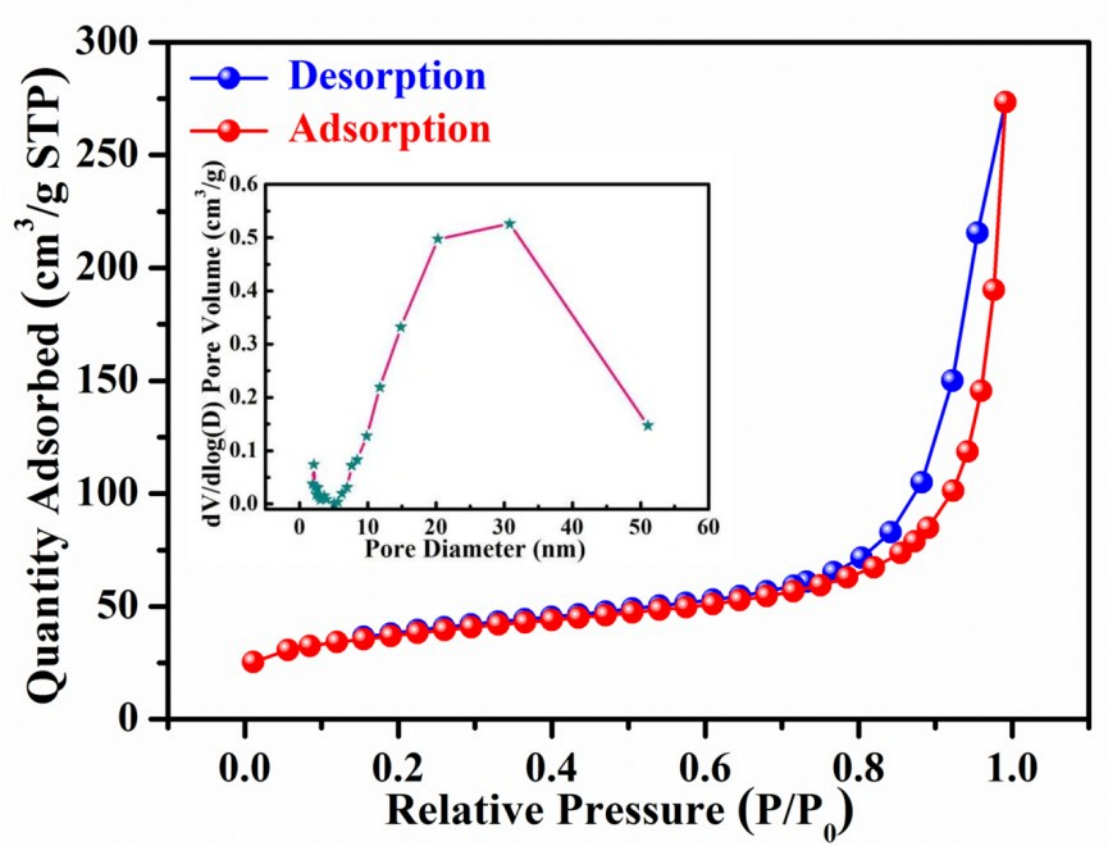

Figure S10 N_2 absorption-desorption isotherm of the S-α-Fe_2O_3 anode material (Inset: BJH desorption pore distribution).

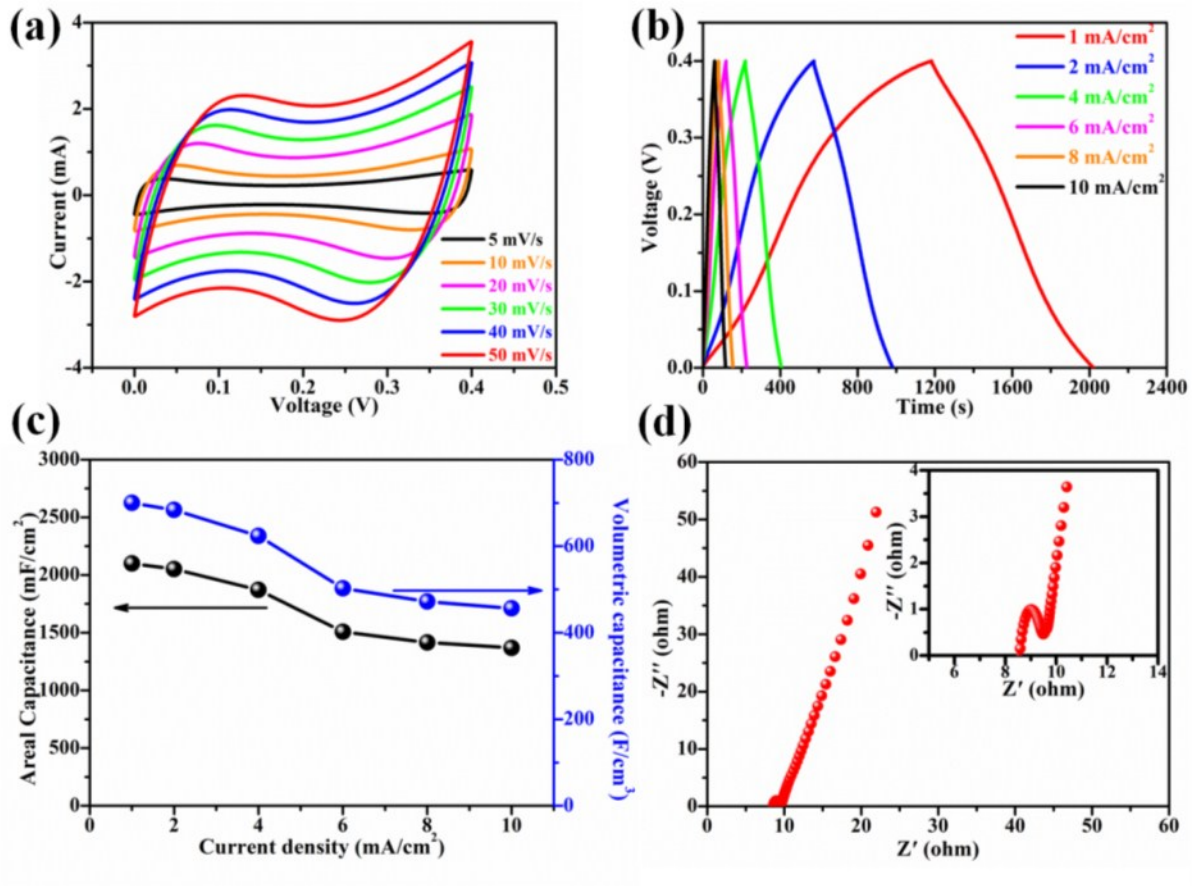

Figure S11 (a) CV curves and (b) GCD curves of the Co_3O_4 NWAs/CNTF electrode.

(c) Specific capacitance and (d) EIS results of the Co_3O_4 NWAs/CNTF electrode.

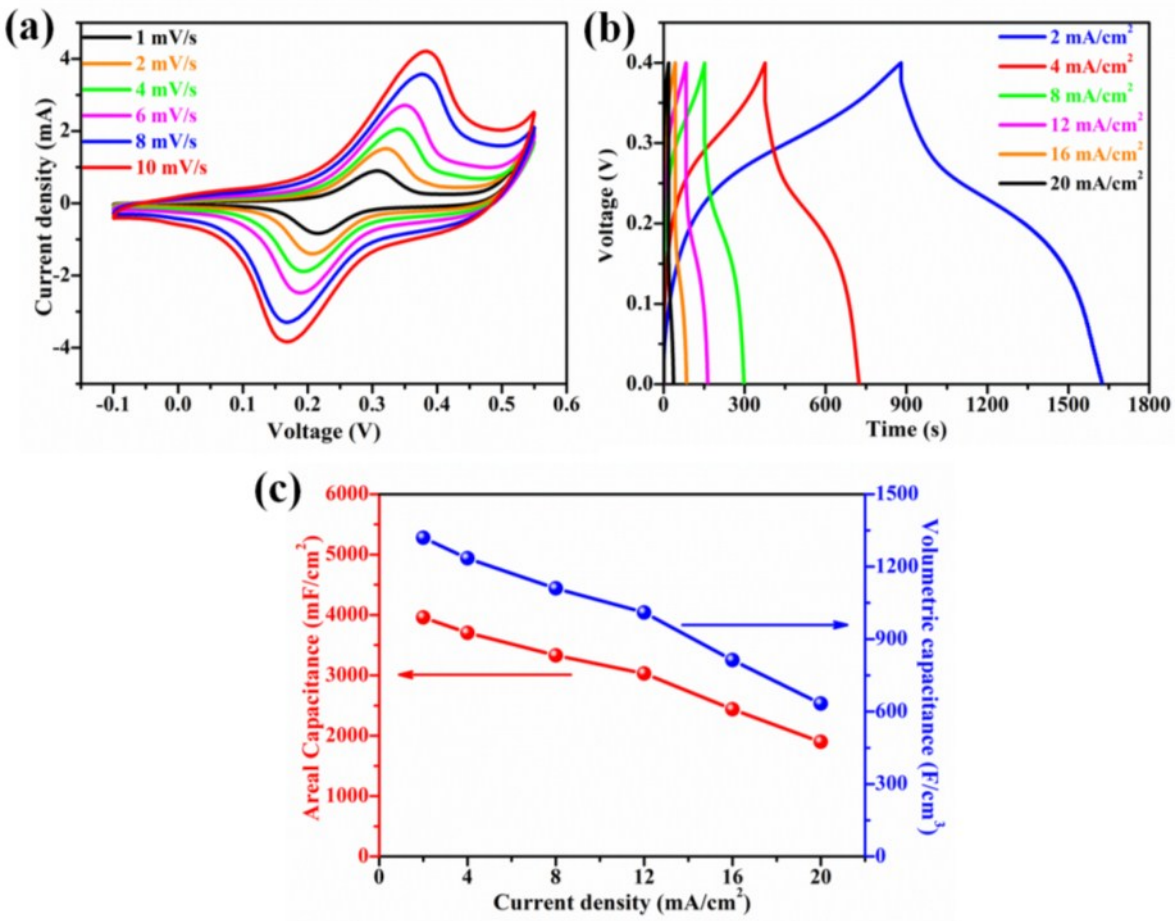

Figure S12 (a) CV curves, (b) GCD curves and (c) specific capacitance of the Co_3O_4@$Ni(OH)_2$ NWAs/CNTF electrode.

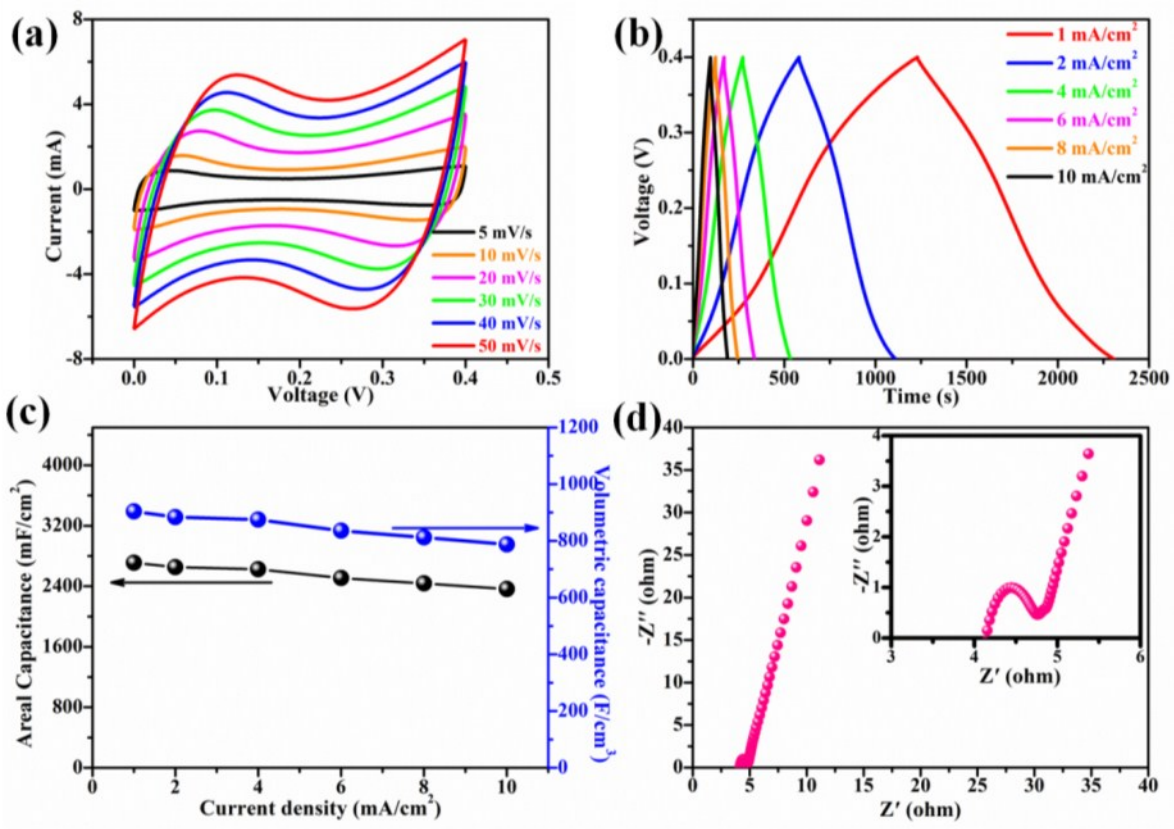

Figure S13 (a) CV curves and (b) GCD curves of the CoP NWAs/CNTF electrode. (c) Specific capacitance and (d) EIS results of the CoP NWAs/CNTF electrode.

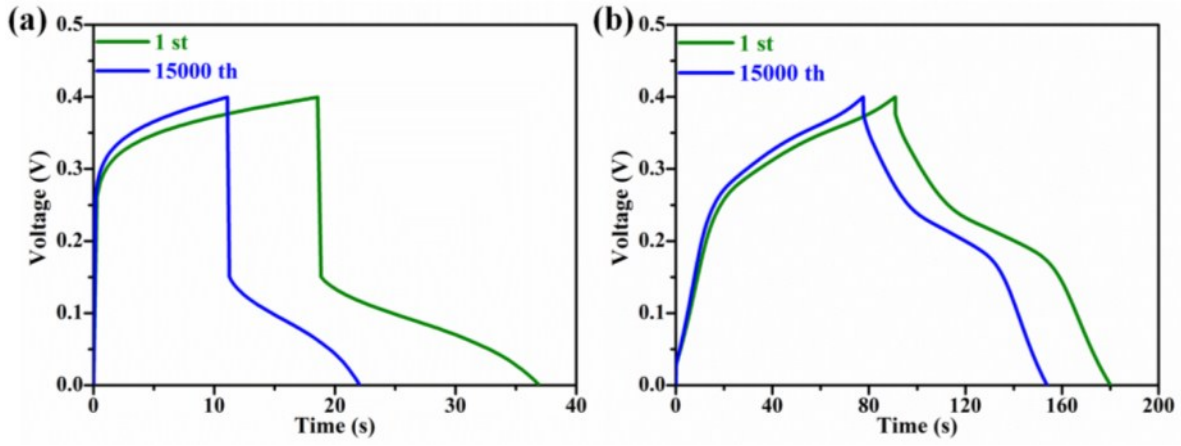

Figure S14 GCD curves for the 1st and 15,000th cycles of (a) Co_3O_4@$Ni(OH)_2$ NWAs/CNTF electrode and (b) CoP@$Ni(OH)_2$ NWAs/CNTF electrode at 20 mA/cm^2.

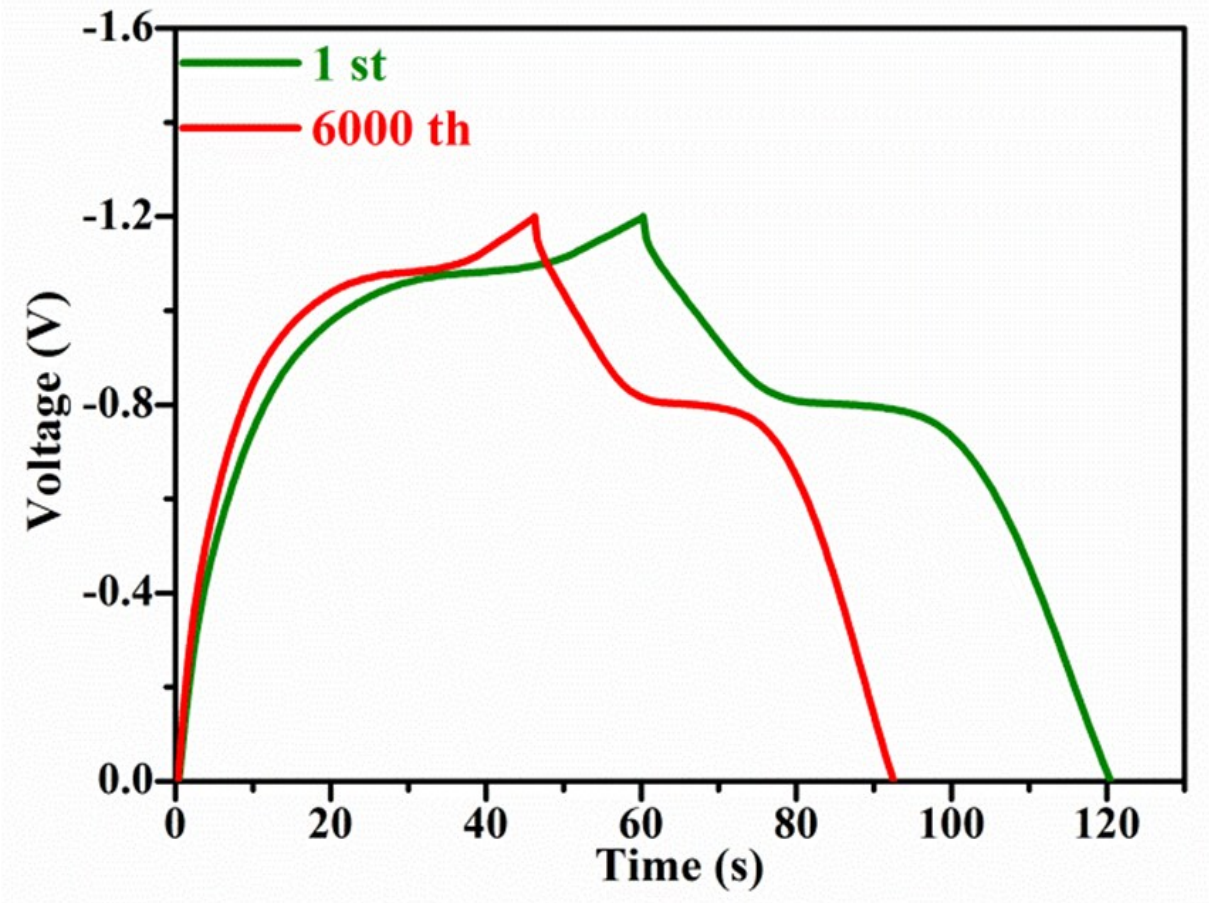

Figure S15 GCD curves for the 1st and 6,000th cycles of the S-α-Fe_2O_3/CNTF electrode.

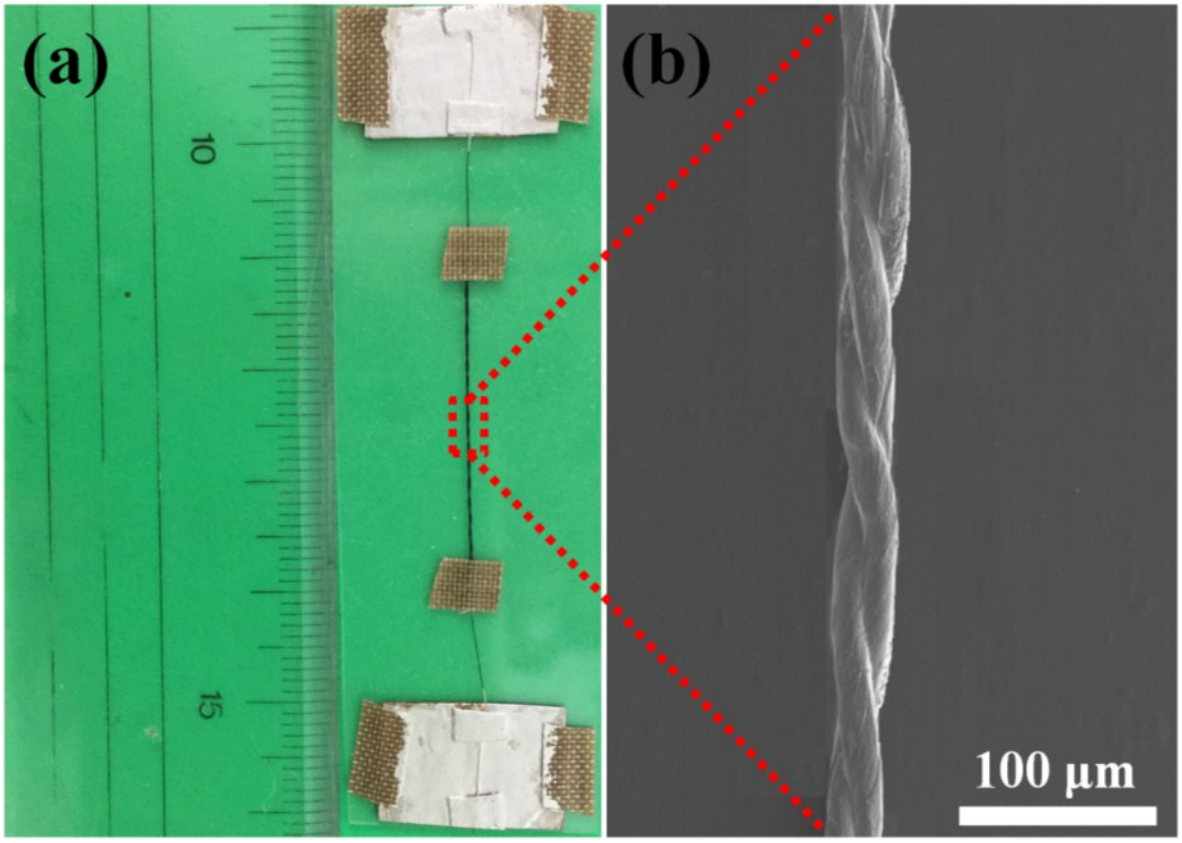

Figure S16 (a) Optical image and (b) SEM image of the as-assembled FESD with twisted structure.

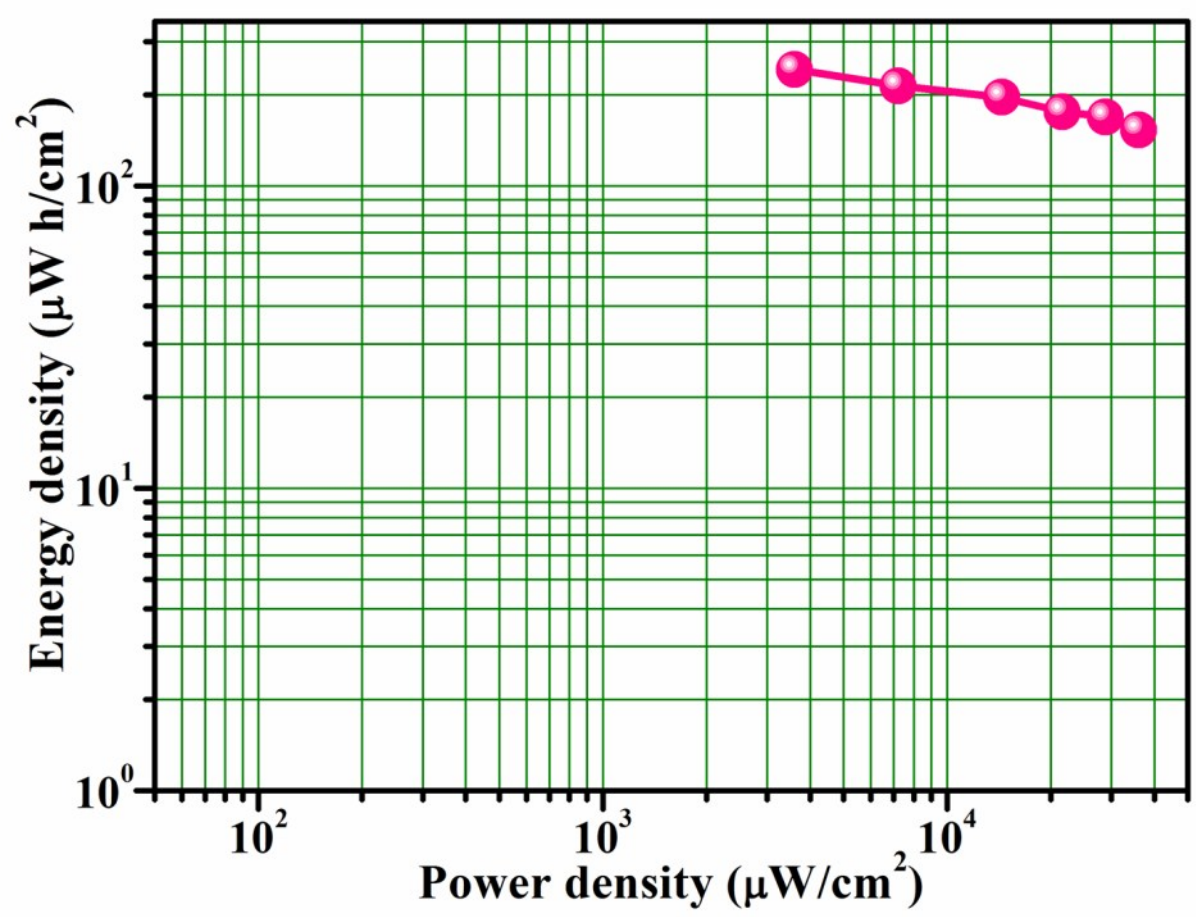

Figure S17 Areal energy and power densities of our as-assembled FESD.

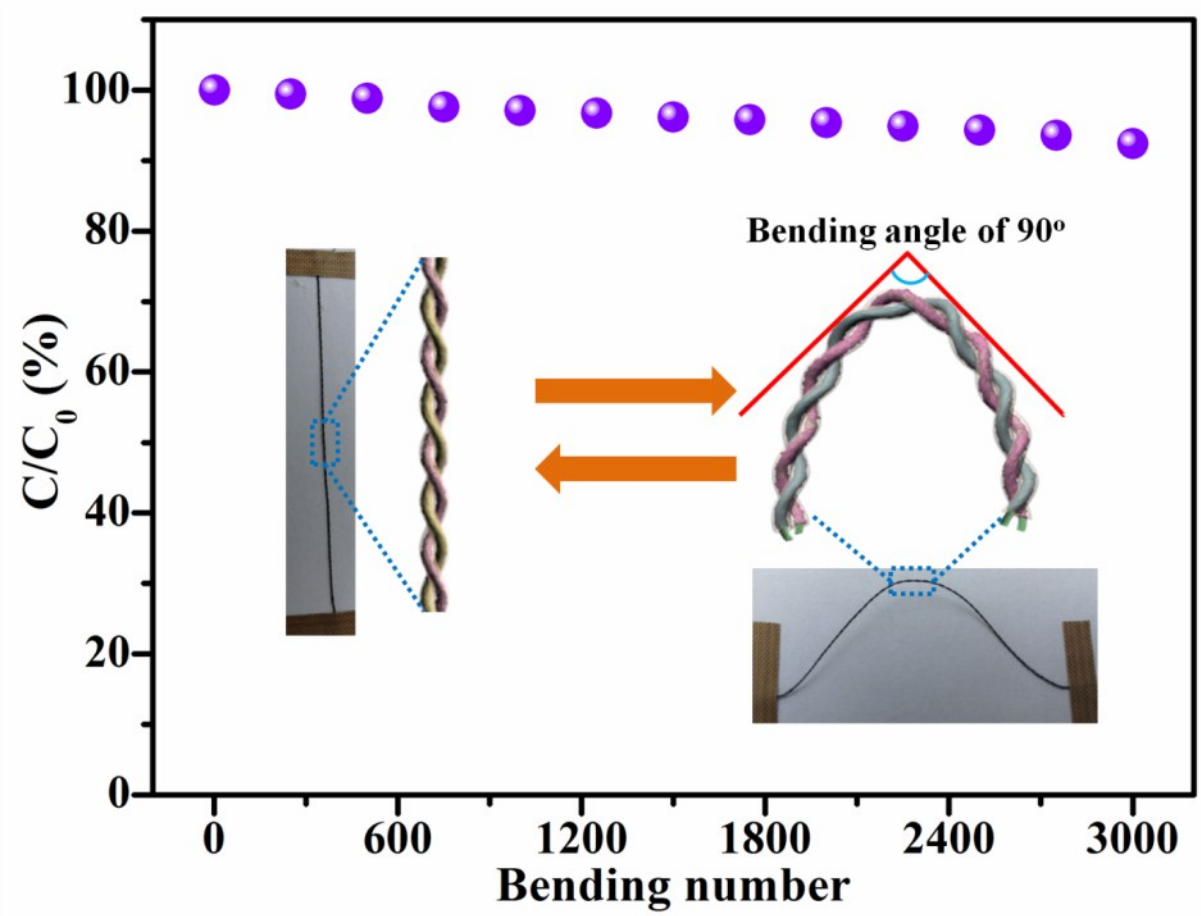

Figure S18 Normalized capacity of the as-assembled FESD bent 90° for 3000 cycles. C_0 is the initial capacity and C is the capacity at the indicated number of bending number.

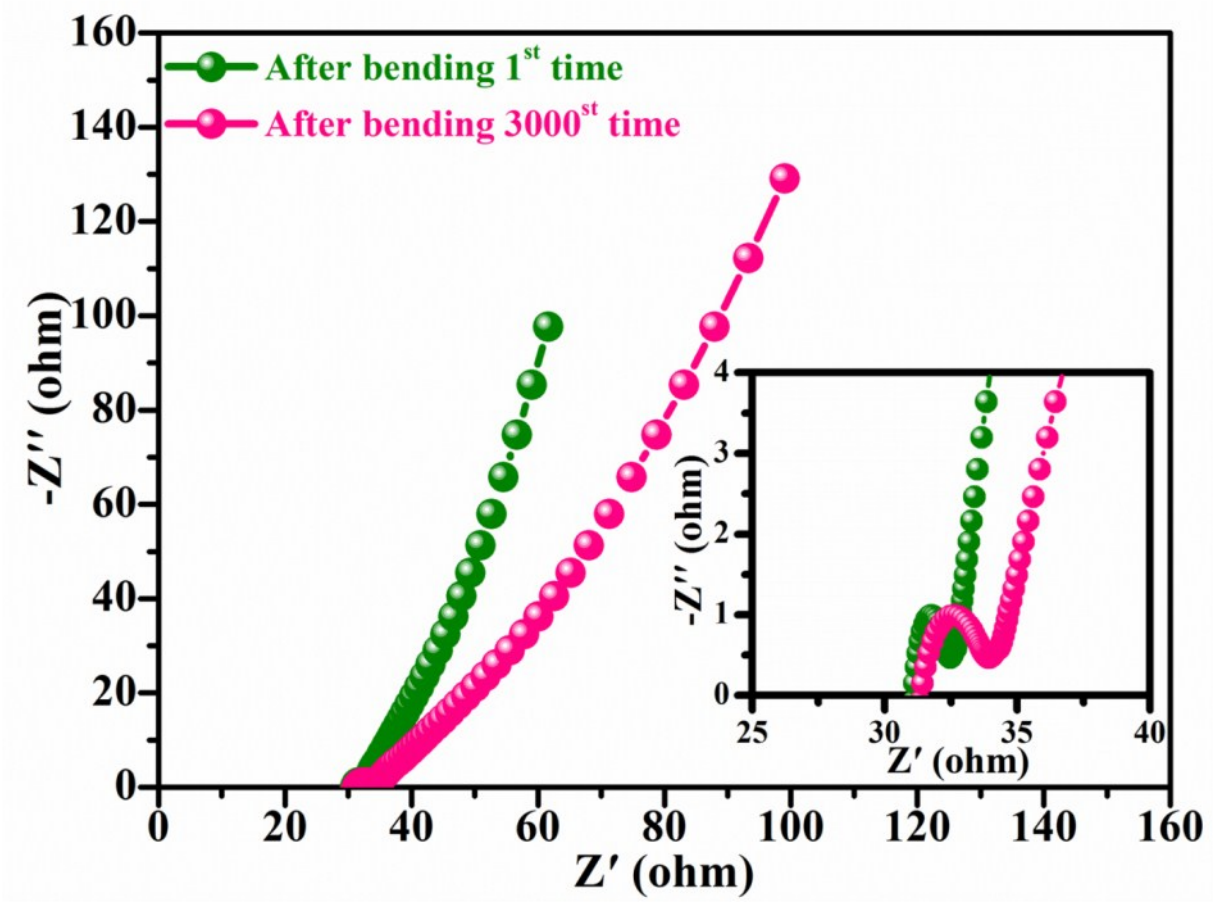

Figure S19 Nyquist plot of the as-assembled FESD at frequencies ranging from 10-2 to 105 Hz with a voltage amplitude of 5 mV at open-circuit potential after bending 1st and 3,000th times.

After the 1st and 3000th bending number, the equivalent series resistance values of our FESD are 31.5 Ω and 32.8 Ω, demonstrating the improvements of the ionic resistance of the electrolyte and the resistance of the electrode material after the bending number. Furthermroe, the semicircle diameter related to charge transfer resistance also increases after 3000 bending numbers.